NASA TECHNICAL NOTE

NASA TN D-3180

NASA TN D-3180

LAUNCHING OF SURFACE WAVES ON AXIAL-CYLINDRICAL REACTIVE SURFACE

by Norman C. Wenger

Lewis Research Center

Cleveland, Ohio

NATIONAL AERONAUTICS AND SPACE ADMINISTRATION • WASHINGTON, D. C. • JANUARY 1966

LAUNCHING OF SURFACE WAVES ON AXIAL-CYLINDRICAL REACTIVE SURFACE

By Norman C. Wenger

Lewis Research Center
Cleveland, Ohio

NATIONAL AERONAUTICS AND SPACE ADMINISTRATION

For sale by the Clearinghouse for Federal Scientific and Technical Information
Springfield, Virginia 22151 – Price $2.00

LAUNCHING OF SURFACE WAVES ON AXIAL-CYLINDRICAL REACTIVE SURFACE

by Norman C. Wenger

Lewis Research Center

SUMMARY

The excitation of the dominant transverse magnetic (TM) surface wave on an axial-cylindrical reactive surface is discussed. The surface wave launcher consists of a perfectly conducting, infinitely thin cylindrical surface coaxial with an axial-cylindrical reactive surface. The reactive surface is of infinite extent, and the perfectly conducting surface is of semi-infinite extent. The surface wave is excited by the dominant TM mode in the coaxial portion of the structure.

Numerical results are obtained for the energy transported by the reflected field, the surface wave field, and the radiation field by using an exact analysis. The exact results are then compared with the results from two approximation techniques that are frequently used to solve problems of this class to determine the validity of these techniques.

This method of excitation was found to be very efficient over a large range of frequencies and over wide variations in the surface reactance.

INTRODUCTION

The propagation of electromagnetic surface waves on various types of structures has been widely treated in the literature. This extensive treatment has been motivated largely by the inherent low attenuation and large bandwidth found in many surface wave structures. Excellent surveys of the properties of surface waves and surface wave structures useful in communications systems have been presented by Zucker (ref. 1) and Barlow (ref. 2). A considerable amount of work on new structures that can support surface waves such as anisotropic ferrites and plasma columns is also being performed. A knowledge of the properties of the surface waves associated with these structures can provide some insight into their composition.

A common problem to all of these areas of interest is the efficient excitation or launching of the guided electromagnetic surface waves. A general requirement for a good surface wave launcher is a high launching efficiency over a large frequency bandwidth. Since the surface wave fields are of infinite extent, the launcher must also be of infinite extent to have 100 percent launching efficiency. Brown (ref. 3) has shown that the launching efficiency of a

finite-sized launcher can be made arbitrarily close to 100 percent. This large efficiency can be realized, however, only at the expense of frequency bandwidth.

A very limited amount of work has been done in analyzing finite-sized launchers that are physically realizable. The majority of numerical data presently available is for the class of launchers that are infinitesimal in some dimension. To this class belong the short electric and magnetic current elements, line sources, current loops, etc. The finite-sized launcher can be handled, at least in theory, by a superposition of infinitesimal sources. In practice, it is usually difficult to carry out this superposition because of the complexity involved in the calculation and the uncertainty in the distribution of the field within the launcher. The finite-sized launcher is usually analyzed by using an approximate field distribution. The field or aperture distribution is often approximated by a "chopped" surface wave distribution; that is, the field in the aperture plane of the launcher is assumed to have the same form as the surface wave field within the aperture and is assumed to vanish everywhere outside of the aperture. Another often-used approximation technique is Kirchhoff's approximation. In this method the aperture field is assumed to be of the same form as the unperturbed incident field. For either case, the surface wave amplitude can be easily computed by an integration over the aperture plane since the surface wave modes and the radiation field are orthogonal (ref. 4). The accuracy of the results obtained by using these approximation techniques is usually unknown since no criterion exists which can determine the extent of the approximations.

The purpose of this report is to present an exact analysis and numerical results for the launching characteristics, radiation pattern, and frequency bandwidth of a finite-sized launcher that is physically realizable. These results will then be compared with the results for the "chopped" surface wave distribution and with the results using Kirchhoff's approximation to determine under what conditions the approximation techniques are valid.

The analysis will be restricted to the class of surface wave structures that have the configuration of a cylindrical column of circular cross section. In order to keep the results of this work as general as possible, the effect of the surface wave structure on the electromagnetic field will be taken into account by specifying a surface impedance. The surface impedance is defined as the ratio of the tangential electric field to the component of the tangential magnetic field perpendicular to the electric field along the surface of the wave guiding structure. The numerical value of the surface impedance will, of course, depend on the composition of the structure and the polarization of the electromagnetic field. The case where the structure has no losses will be considered to simplify the analysis; consequently, the surface impedance will be a pure reactance. Only the case of inductive surface reactance will be treated.

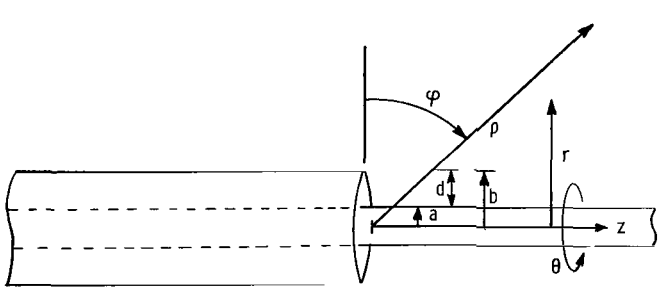

Figure 1. - Surface wave structure.

The particular configuration

that will be considered is shown in figure 1. The structure consists of a reactive cylindrical surface of radius a and of infinite extent in the z-direction. Coaxial with this cylinder is an infinitely thin, perfectly conducting surface of radius b for $z < 0$. The surface wave field, radiation field, and the reflected field will be computed for the case where the incident field is the dominant transverse magnetic (TM) mode in the region $a < r < b$ and $z < 0$, propagating in the positive z-direction. The analysis will be restricted to the frequency range where the dominant TM mode is the only propagating mode.

Before a formal solution of the problem is carried out it is instructive to examine the various types of waves that exist in the different portions of the structure.

SYMBOLS

a	radius of cylindrical reactive surface (see fig. 1)
b	radius of perfectly conducting surface (see fig. 1)
d	b-a (see fig. 1)
$E^{+}(b,\beta)$	function defined in eq. (18c)
$F(\beta)$	function defined in eq. (21)
$F^{\pm}(\beta)$	Weiner-Hopf factors of $F(\beta)$
h_o	eigenvalue for surface wave mode
Im	imaginary part of
$J^{+}(b,\beta)$	function defined in eq. (18a)
$J^{-}(b,\beta)$	function defined in eq. (18b)
j	$\sqrt{-1}$
k_o	free-space wave number
k_o'	real part of k_o
k_o''	negative imaginary part of k_o
p_n	eigenvalue of coaxial mode
Re	real part of
r	radial coordinate (see fig. 1)
X_s	surface reactance

Z_o	characteristic impedance of free space
z	axial coordinate (see fig. 1)
α	$k_o X_s / Z_o$
β	complex variable
β_o	propagation constant for surface wave mode
β_o'	real part of β_o
β_o''	negative imaginary part of β_o
γ_n	propagation constant for coaxial mode
γ_o'	real part of γ_o
γ_o''	negative imaginary part of γ_o
θ	azimuthal angle (see fig. 1)
ρ	radial coordinate (see fig. 1)
φ	compliment of polar angle (see fig. 1)
$\varphi(r,\beta)$	Fourier transform of $\psi(r,z)$
$\varphi^{\pm}(r,\beta)$	single-sided Fourier transforms of $\psi(r,z)$
$\psi(r,z)$	θ component of total magnetic field
$\psi_i(r,z)$	incident field
$\psi_s(r,z)$	scattered field
ω	angular frequency

Subscripts:

i	incident
rad	radiated
rf	reflected
sw	surface wave

SURFACE WAVE LAUNCHER

Coaxial Portion of Structure

The total field in the coaxial portion of the structure can be expressed in the form of an infinite summation of modes. These modes will consists, in general, of transverse magnetic (TM), transverse electric (TE), and hybrid modes. The characteristics of these modes will depend on the variation of the surface reactance with frequency and on the polarization of the field.

At low frequencies only the TM_{oo} mode will propagate. The subscripts denoting the TM_{mn} modes are selected such that the first subscript m corresponds to the number of cyclic variations of the mode intensity with θ and the second subscript n corresponds to the number of nodes of the mode intensity with radius. The TM_{oo} mode is composed of an electric field with axial and radial components and a magnetic field with an azimuthal component. All other field components are zero. The remaining TM modes and all the TE and hybrid modes are cut off at low frequencies. Thus, the total field in the coaxial portion of the structure will consist of the TM_{oo} mode except in the vicinity of the discontinuity at $z = 0$. The presence of the discontinuity will cause the dominant TM_{oo} mode to excite the evanescent TM_{on} modes. All the other possible modes are not excited since both the TM_{oo} mode and the discontinuity are circularly symmetric. The total field in the coaxial portion of the structure will consist, therefore, of the entire spectrum of TM_{on} modes with each mode having an axial and radial component of electric field and an azimuthal component of magnetic field. Since the electric and magnetic fields are related by Maxwell's equations, only the magnetic field need be determined to uniquely specify the total field. Thus, the azimuthal or θ component of the magnetic field can be regarded as a scalar function from which all the other field components can be derived.

Let $\psi(r,z)$ be the θ component of the magnetic field. Then, in the coaxial portion of the structure, $\psi(r,z)$ can be expanded in a series of the eigenfunctions (ref. 5, pp. 709 to 778):

$$\psi(r,z) = A_o\left[J_1(-jp_or)H_0^2(-jp_ob) - J_0(-jp_ob)H_1^2(-jp_or)\right]e^{-j\gamma_o z} + \sum_{n=1}^{\infty} A_n\left[J_1(p_nr)H_0^2(p_nb) - J_0(p_nb)H_1^2(p_nr)\right]e^{-\gamma_n z} \qquad (1)$$

where the A_n are complex amplitude constants. A time dependence of $e^{j\omega t}$ has been assumed for all field quantities. Since the solution (1) must satisfy Maxwell's equations, the eigenvalues p_n and the propagation constants γ_n are related by

$$\gamma_o^2 = p_o^2 + k_o^2$$

$$\gamma_n^2 = p_n^2 - k_o^2 \qquad \text{for} \quad n > 0$$

where k_o is the free-space wave number. The eigenvalues p_n are determined by the boundary conditions. The ratio of the axial component of the electric field to the azimuthal component of the magnetic field must equal the surface reactance jX_s along the reactive surface $r = a$. This condition requires $\psi(r,z)$ to satisfy the equation

$$\frac{1}{r}\frac{\partial}{\partial r}\left[r\psi(r,z)\right] + \alpha\psi(r,z)\Big|_{r=a} = 0 \tag{2}$$

where $\alpha \equiv k_o X_s/Z_o$ and Z_o is the characteristic impedance of free space. Substituting the general solution (1) into equation (2) generates the following set of equations that must be satisfied by the eigenvalues p_n:

$$jp_o a\,\frac{J_0(-jp_o b)H_0^2(-jp_o a) - J_0(-jp_o a)H_0^2(-jp_o b)}{J_1(-jp_o a)H_0^2(-jp_o b) - J_0(-jp_o b)H_1^2(-jp_o a)} = -\alpha a \tag{3a}$$

$$p_n a\,\frac{N_0(p_n b)J_0(p_n a) - J_0(p_n b)N_0(p_n a)}{J_0(p_n b)N_1(p_n a) - N_0(p_n b)J_1(p_n a)} = \alpha a \qquad \text{for} \quad n > 0 \tag{3b}$$

Along the surface of the perfect conductor $r = b$, the axial component of the electric field must vanish. This condition requires $\psi(r,z)$ to satisfy the equation

$$\frac{1}{r}\frac{\partial}{\partial r}\left[r\psi(r,z)\right]\Big|_{r=b} = 0 \tag{4}$$

This boundary condition has been built into solution (1).

If the surface reactance vanishes, the first term in solution (1) will reduce to the ordinary TEM wave associated with a coaxial line; whereas the remaining terms in solution (1) will reduce to the TM_{on} modes for a coaxial line. It should also be noted that since the total field consists entirely of TM modes it is only necessary to specify the surface reactance for one polarization of the electric field. The value of the surface reactance for other polarizations is arbitrary.

Open Portion of Structure

The total field in the open portion of the structure consists of discrete modes guided by the reactive surface plus the radiation field. The guided waves can be described as either TM, TE, or hybrid. Since the field in the coaxial portion of the structure is composed entirely of circularly symmetric TM modes and since the structure is circularly symmetric, the field in the open portion of the structure will also consist of circularly symmetric TM modes. The only transverse magnetic mode that possesses circular symmetry is the TM_o mode, which is commonly called the Goubau wave. The single subscript n denoting the various TM_n modes refers to the number of cyclic variations of the

mode intensity with θ. A second subscript is not necessary since all modes in the open portion of the structure are evanescent in the radial direction.

The total field $\psi(r,z)$ in the open portion of the structure consists, therefore, of the radiation field plus the TM_o surface wave (ref. 2, pp. 60 to 69) of the form

$$B_o H_1^2(-jh_o r)e^{-j\beta_o z} \tag{5}$$

where B_o is a complex amplitude constant. The eigenvalue h_o and the propagation constant β_o are related by

$$\beta_o^2 = h_o^2 + k_o^2$$

since equation (5) must satisfy Maxwell's equations. The eigenvalue h_o is determined by the boundary condition (2) at the reactive surface. Substituting equation (5) into equation (2) requires h_o to satisfy the equation

$$jh_o a \frac{H_0^2(-jh_o a)}{H_1^2(-jh_o a)} = \alpha a \tag{6}$$

FORMAL SOLUTION OF PROBLEM

Statement of Problem

The formal solution of the problem will be carried out by using Laplace transform and Wiener-Hopf (refs. 6 and 7) techniques. It is convenient to decompose the total field $\psi(r,z)$ into two parts: an incident field $\psi_i(r,z)$ and a scattered field $\psi_s(r,z)$, where

$$\psi(r,z) = \psi_i(r,z) + \psi_s(r,z)$$

The incident field is the dominant TM_{oo} mode in the coaxial portion of the structure and exists by definition for $a < r < b$ and all values of z:

$$\psi_i(r,z) \equiv \frac{\pi p_o b}{2}\left[J_1(-jp_o r)H_0^2(-jp_o b) - J_0(-jp_o b)H_1^2(-jp_o r)\right]e^{-j\gamma_o z} \tag{7}$$

The amplitude factor in equation (7) has been selected such that the incident field has unit amplitude at $r = b$. Since the incident field does not satisfy the proper boundary conditions for $z > 0$, the scattered field will contain a term of the same form as the incident field for $z > 0$ to nullify this improper solution.

The scattered field satisfies the following equations:

$$\frac{\partial^2\psi_s}{\partial r^2} + \frac{1}{r}\frac{\partial\psi_s}{\partial r} + \frac{\partial^2\psi_s}{\partial z^2} + \left(k_o^2 - \frac{1}{r^2}\right)\psi_s = 0 \tag{8}$$

$$\frac{1}{r}\frac{\partial}{\partial r}(r\psi_s) + \alpha\psi_s \Big|_{r=a} = 0 \tag{9}$$

$$\frac{1}{r}\frac{\partial}{\partial r}(r\psi_s) \Big|_{\substack{r=b \\ z<0}} = 0 \tag{10}$$

$$\psi_s \Big|_{\substack{r=b^+ \\ z>0}} - \psi_s \Big|_{\substack{r=b^- \\ z>0}} = e^{-j\gamma_o z} \tag{11}$$

$$\frac{1}{r}\frac{\partial}{\partial r}(r\psi_s) \Big|_{\substack{r=b^+ \\ z>0}} - \frac{1}{r}\frac{\partial}{\partial r}(r\psi_s) \Big|_{\substack{r=b^- \\ z>0}} = 0 \tag{12}$$

Equation (8) is the Helmholtz equation expressed in cylindrical coordinates. Equations (9) and (10) are a statement of the boundary conditions on the reactive surface and on the perfectly conducting surface, respectively. Equation (11) requires the scattered field to be discontinuous at $r = b$ and $z > 0$ in order to make the total field continuous. Equation (12) requires the axial component of the electric field to be continuous at $r = b$ and $z > 0$. In addition to the above boundary conditions, a radiation condition must also be imposed. The radiation condition requires all admissible solutions for the scattered field to correspond to divergent waves at infinity.

Laplace Transformation

Let the function $\varphi(r,\beta)$ be defined by

$$\varphi(r,\beta) \equiv \varphi^+(r,\beta) + \varphi^-(r,\beta)$$

where

$$\varphi^+(r,\beta) \equiv \int_0^\infty \psi_s(r,z)e^{-\beta z}\,dz$$

and

$$\varphi^-(r,\beta) \equiv \int_{-\infty}^{0} \psi_s(r,z)e^{-\beta z}\, dz$$

The scattered field $\psi_s(r,z)$ can then be recovered by the inversion integral

$$\psi_s(r,z) = \frac{1}{2\pi j}\int_C \varphi(r,\beta)e^{\beta z}\, d\beta$$

where C denotes a suitable contour in the complex β-plane.

In order to make $\varphi^+(r,\beta)$ and $\varphi^-(r,\beta)$ analytic functions of β in a common region in the complex β-plane, the free-space wave number k_o will be made complex. This is equivalent to introducing losses into the medium surrounding the structure. Let $jk_o = jk_o' + k_o''$, where k_o' and k_o'' are real. In the final solution k_o'' will be set equal to zero to recover the result for the lossless case. Since k_o is complex, the propagation constants γ_o and β_o will also be complex. Thus, γ_o and β_o will, in general, be given by $j\gamma_o = j\gamma_o' + \gamma_o''$ and $j\beta_o = j\beta_o' + \beta_o''$, where γ_o', γ_o'', β_o', and β_o'' are all real. The inequalities $k_o' \le \beta_o' \le \gamma_o'$ and $\gamma_o'' \le \beta_o'' \le k_o''$ can be shown to be valid for all cases.

Taking the Laplace transform of equations (8), (9), and (10) gives

$$\frac{\partial^2\varphi}{\partial r^2} + \frac{1}{r}\frac{\partial\varphi}{\partial r} + \left(\beta^2 + k_o^2 - \frac{1}{r^2}\right)\varphi = 0 \tag{13}$$

$$\frac{1}{r}\frac{\partial}{\partial r}(r\varphi) + \alpha\varphi \Big|_{r=a} = 0 \tag{14}$$

$$\frac{1}{r}\frac{\partial}{\partial r}(r\varphi^-) \Big|_{r=b} = 0 \tag{15}$$

where β by virtue of the previous discussion, must be restricted to the range $-\gamma_o'' < \mathrm{Re}\ \beta < \gamma_o''$.

Solution for Transformed Scattered Field

The solution of equation (13) is of the form

$$\varphi(r,\beta) = A(\beta)J_1(\lambda r) + B(\beta)H_1^2(\lambda r)$$

where $\lambda \equiv (k_0^2 + \beta^2)^{1/2}$ and $A(\beta)$ and $B(\beta)$ are suitable functions of β that must be selected to satisfy the boundary conditions (14) and (15) and the radiation condition.

In the region $a < r < b$ the proper solution of equation (13) is

$$\varphi(r,\beta) = \varphi(b^-,\beta) \frac{\left[\lambda H_0^2(\lambda a) + \alpha H_1^2(\lambda a)\right] J_1(\lambda r) - \left[\lambda J_0(\lambda a) + \alpha J_1(\lambda a)\right] H_1^2(\lambda r)}{\left[\lambda H_0^2(\lambda a) + \alpha H_1^2(\lambda a)\right] J_1(\lambda b) - \left[\lambda J_0(\lambda a) + \alpha J_1(\lambda a)\right] H_1^2(\lambda b)} \tag{16}$$

The solution given by equation (16) is an even function of λ; consequently, either branch of λ can be selected. In the region $r > b$ the proper solution of equation (13) is

$$\varphi(r,\beta) = \varphi(b^+,\beta) \frac{H_1^2(\lambda r)}{H_1^2(\lambda b)} \tag{17}$$

In order to satisfy the radiation condition, the branch of λ where $\operatorname{Im} \lambda < 0$ must be selected.

The unknown coefficients $\varphi(b^-,\beta)$ and $\varphi(b^+,\beta)$ in equations (16) and (17) can be determined by the discontinuity condition on the scattered field at $r = b$ as given by equation (11). This can easily be accomplished by introducing the functions $J^+(b,\beta)$, $J^-(b,\beta)$ and $E^+(b,\beta)$, where

$$J^+(b,\beta) \equiv \int_0^\infty \left[\psi_s(b^+,z) - \psi_s(b^-,z)\right] e^{-\beta z}\, dz \tag{18a}$$

$$J^-(b,\beta) \equiv \int_{-\infty}^0 \left[\psi_s(b^+,z) - \psi_s(b^-,z)\right] e^{-\beta z}\, dz \tag{18b}$$

$$E^+(b,\beta) \equiv \frac{1}{r} \frac{\partial}{\partial r} (r\varphi) \Bigg|_{r=b} \tag{18c}$$

It should be noted that the function $J^-(b,\beta)$ is actually the Laplace transform of the portion of the electric current on the perfectly conducting surface $r = b$ associated with the scattered field. The function $E^+(b,\beta)$ is proportional to the transform of the axial component of the total electric field evaluated at $r = b$. Thus, $E^+(b,\beta)$ could have been defined equally well by the equation

$$E^+(b,\beta) = \frac{1}{r} \frac{\partial}{\partial r} (r\varphi^+) \Bigg|_{r=b}$$

by virtue of equation (15). The function $J^+(b,\beta)$ can be calculated at once for for the region $\mathrm{Re}\ \beta > -\gamma_o''$ by using equation (11):

$$J^+(b,\beta) = \frac{1}{\beta + j\gamma_o} \tag{19}$$

The functions $J^-(b,\beta)$ and $E^+(b,\beta)$ are, at present, unknown; however, a consideration of the complex forms of k_o, β_o, and γ_o reveals that $J^-(b,\beta)$ is an analytic function of the complex variable β in the region $\mathrm{Re}\ \beta < \gamma_o''$ and that $E^+(b,\beta)$ is analytic in the region $\mathrm{Re}\ \beta > -\gamma_o''$.

From the definitions of $J^+(b,\beta)$ and $J^-(b,\beta)$ it is apparent that

$$\varphi(b^+,\beta) - \varphi(b^-,\beta) = J^+(b,\beta) + J^-(b,\beta) \tag{20}$$

The unknown coefficients $\varphi(b^-,\beta)$ and $\varphi(b^+,\beta)$ can be expressed in terms of the function $E^+(b,\beta)$ by using the solutions (16) and (17) in conjunction with the definition for $E^+(b,\beta)$ as given by equation (18c). The result of this operation allows the left side of equation (20) to be put into the form

$$\varphi(b^+,\beta) - \varphi(b^-,\beta) = F(\beta)E^+(b,\beta) \tag{21}$$

where $F(\beta)$ is given by

$$F(\beta) \equiv \frac{2j}{\pi b\lambda^2} \frac{H_0^2(\lambda a)}{H_0^2(\lambda b)} \left[\lambda + \alpha \frac{H_1^2(\lambda a)}{H_0^2(\lambda a)}\right]$$

$$\times \frac{1}{\lambda\left[H_0^2(\lambda a)J_0(\lambda b) - H_0^2(\lambda b)J_0(\lambda a)\right] + \alpha\left[H_1^2(\lambda a)J_0(\lambda b) - H_0^2(\lambda b)J_1(\lambda a)\right]}$$

The function $F(\beta)$ can be shown to be analytic in the strip $-\gamma_o'' < \mathrm{Re}\ \beta < \gamma_o''$. Substituting equation (21) into equation (20) and using the result for $J^+(b,\beta)$ from equation (19) give

$$F(\beta)E^+(b,\beta) = J^-(b,\beta) + \frac{1}{\beta + j\gamma_o} \tag{22}$$

Wiener-Hopf factorization. - Equation (22) can be solved for the functions $E^+(b,\beta)$ and $J^-(b,\beta)$ by performing a Wiener-Hopf factorization on the function $F(\beta)$; that is, $F(\beta)$ will be expressed as the ratio of the two functions $F^+(\beta)$ and $F^-(\beta)$, where $F^+(\beta)$ is analytic and nonzero for $\mathrm{Re}\ \beta > -\gamma_o''$ and $F^-(\beta)$ is analytic and nonzero for $\mathrm{Re}\ \beta < \gamma_o''$. The details of this factorization are given in the appendix. It is sufficient, at this point to list some of the properties of the functions $F^+(\beta)$ and $F^-(\beta)$:

(1) The function $F^+(\beta)$ has a single zero at $\beta = -j\beta_o$ and a branch point at $\beta = -jk_o$.

(2) The function $F^-(\beta)$ has an infinite number of zeros in the complex β-plane and a branch point at $\beta = jk_o$. The zeros of $F^-(\beta)$ are located at $\beta = j\gamma_o$ and $\beta = \gamma_n (n > 0)$.

(3) The function $F^+(\beta)$ is of the order $\beta^{-1/2}$ at infinity, and the function $F^-(\beta)$ is of the order $\beta^{1/2}$ at infinity.

The decomposition of the function $F(\beta)$ into the ratio of $F^+(\beta)$ to $F^-(\beta)$ allows equation (22) to be put into the form

$$F^+(\beta)E^+(b,\beta) - \frac{F^-(-j\gamma_o)}{\beta + j\gamma_o} = \frac{F^-(\beta) - F^-(-j\gamma_o)}{\beta + j\gamma_o} + F^-(\beta)J^-(b,\beta) \qquad (23)$$

Figure 2 shows the regions in the complex β-plane where the various transforms are analytic. A study of figure 2 reveals that the left side of equation (23) is analytic for $\text{Re}\,\beta > -\gamma_o''$ and that the right side is analytic for $\text{Re}\,\beta < \gamma_o''$. The equality in equation (23) holds only in the strip $-\gamma_o'' < \text{Re}\,\beta < \gamma_o''$.

Edge conditions. - The solution for the scattered field is not unique unless the edge conditions are specified at $r = b$ and $z = 0$ (ref. 7, pp. 75 to 76). These conditions require the axial component of the electric field to be of the order of $z^{-1/2}$ at the edge, which makes the transform of the electric field (i.e., $E^+(b,\beta)$) of the order of $\beta^{-1/2}$ as $\beta \to \infty$. A similar condition exists for the asymptotic form of the current at the edge. This condition requires $J^-(b,\beta)$ to be of the order of β^{-1} as $\beta \to -\infty$.

The asymptotic forms of $F^+(\beta)$, $F^-(\beta)$, $E^+(b,\beta)$, and $J^-(b,\beta)$ for large values of β show that each side of equation (23) approaches zero as β goes to infinity in the proper half plane. A function that is analytic everywhere in the complex β-plane can be defined from equation (23). This function is equal to the left side of equation (23) for $\text{Re}\,\beta > -\gamma_o''$, the right side of equation (23) for $\text{Re}\,\beta < \gamma_o''$, and either side of equation (23) in the strip $-\gamma_o'' < \text{Re}\,\beta < \gamma_o''$. Liouville's theorem (ref. 5, pp. 381 to 382) requires this function to be zero since zero is the only function that is analytic everywhere in the complex β-plane and vanishes at infinity. Setting the left side of equation (23) equal to zero gives

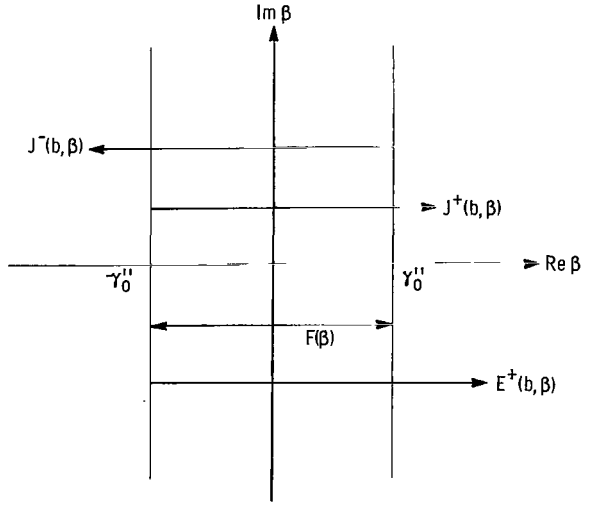

Figure 2. - Regions in complex β-plane where transforms are analytic.

$$E^+(b,\beta) = \frac{F^-(-j\gamma_o)}{F^+(\beta)(\beta + j\gamma_o)} \qquad (24)$$

Note that the proper edge conditions for $E^+(b,\beta)$ are satisfied by equation (24).

Transformed scattered field. - The coefficients $\varphi(b^-,\beta)$ and $\varphi(b^+,\beta)$ can now be expressed in terms of the known function $E^+(b,\beta)$ by using equations (16), (17), and (18c):

$$\varphi(b^-,\beta) = \frac{H_1^2\left(\sqrt{k_o^2 + \beta^2}\, b\right)F^-(-j\gamma_o)}{\left(k_o^2 + \beta^2\right)^{1/2} H_0^2\left(\sqrt{k_o^2 + \beta^2}\, b\right)F^+(\beta)(\beta + j\gamma_o)} - \frac{F^-(-j\gamma_o)}{F^-(\beta)(\beta + j\gamma_o)} \tag{25}$$

$$\varphi(b^+,\beta) = \frac{F^-(-j\gamma_o)H_1^2\left(\sqrt{k_o^2 + \beta^2}\, b\right)}{\left(k_o^2 + \beta^2\right)^{1/2} F^+(\beta)H_0^2\left(\sqrt{k_o^2 + \beta^2}\, b\right)(\beta + j\gamma_o)} \tag{26}$$

Combining the expressions for $\varphi(b^-,\beta)$ and $\varphi(b^+,\beta)$ with the solutions (16) and (17), respectively, completes the solution for the transformed scattered magnetic field.

Scattered Field

Inversion integral. - The scattered magnetic field $\psi_s(r,z)$ can now be computed by using the inversion integral

$$\psi_s(r,z) = \frac{1}{2\pi j}\int_C \varphi(r,\beta)e^{\beta z}\, d\beta$$

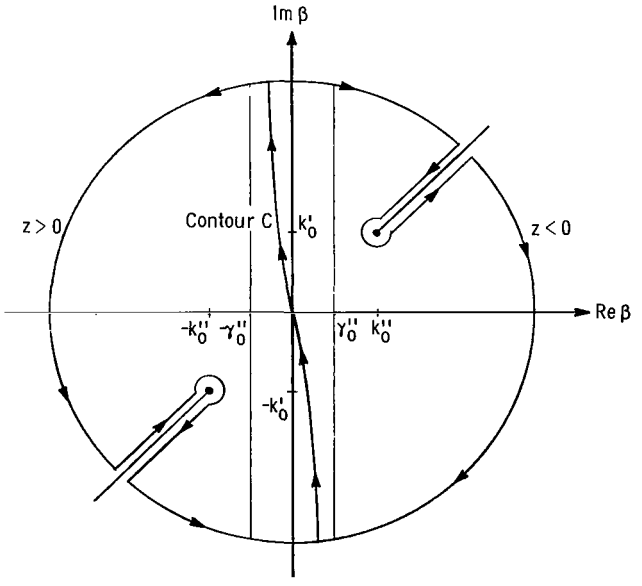

Figure 3. - Inversion contour in complex β-plane.

The inversion contour C must be located in the strip $-\gamma_o'' < \mathrm{Re}\ \beta < \gamma_o''$, as shown in figure 3, and be on the sheet of the Riemann surface that corresponds to the choice $\mathrm{Im}(k_o^2 + \beta^2)^{1/2} < 0$ in this strip. The branch cuts were selected as straight line segments extending radially from the branch points $\beta = \pm jk_o$. For the lossless case the branch cuts will be located on the imaginary β-axis.

Discrete spectrum. - In the computation of the discrete portion of the spectrum, the amplitudes of the modes need be evaluated at only one radius since the radial variation of these modes is already known. It is convenient to evaluate the field at the radius $r = b$ since the radially

varying factor in the general solutions (16) and (17) has been normalized to unity at $r = b$.

First, consider the region $a < r < b$ and $z < 0$. The amplitude of the scattered field at $r = b$ is

$$\psi_s(b,z) = \frac{1}{2\pi j} \int_C \varphi(b^-,\beta) e^{\beta z} \, d\beta$$

where $\varphi(b^-,\beta)$ is given by equation (25). The contour C can be closed in the right half β-plane with a semicircle of infinite radius that is deformed around the branch cut as shown in figure 3. The integration along the semicircle and along the branch cut can be shown to be zero for $z < 0$. Thus, the integral over the original contour C must equal $-2\pi j$ times the sum of the residues of the enclosed poles in the right half β-plane. All of the poles of $\varphi(b^-,\beta)$ in the right half β-plane are due to the zeros of $F^-(\beta)$. Thus, for $z < 0$

$$\psi_s(b,z) = \frac{F^-(-j\gamma_o)}{2j\gamma_o \left.\frac{\partial F^-(\beta)}{\partial \beta}\right|_{\beta=j\gamma_o}} e^{j\gamma_o z} + \sum_{n=1}^{\infty} \frac{F^-(-j\gamma_o)}{(\gamma_n + j\gamma_o) \left.\frac{\partial F^-(\beta)}{\partial \beta}\right|_{\beta=\gamma_n}} e^{\gamma_n z} \qquad (27)$$

The first term in equation (27) represents the dominant TM_{oo} mode in the reflected field, and the summation represents the evanescent TM_{on} modes in the reflected field. In the region $a < r < b$ and $z \ll 0$ the reflected field consists entirely of the first term, the TM_{oo} mode.

The field in the region $z > 0$ evaluated at $r = b$ can be found by using the same inversion integral. This time, however, the contour is closed in the left half β-plane with a semicircle of infinite radius that is deformed around the branch cut. The integration along the semicircle can be shown to be zero for $z > 0$. Thus, the integral over the original contour C must equal $2\pi j$ times the sum of the residues of the enclosed poles in the left half β-plane plus the branch cut integral. The poles of $\varphi(b^-,\beta)$ in the left half β-plane are due to the zero of $F^+(\beta)$ at $\beta = -j\beta_o$ and the pole appearing explicitly in equation (25) at $\beta = -j\gamma_o$. Thus, for $z > 0$

$$\psi_s(b,z) = \frac{-jH_1^2(-jh_o b)F^-(-j\gamma_o)}{(k_o^2 - \beta_o^2)^{1/2} H_0^2(-jh_o b)(\gamma_o - \beta_o) \left.\frac{\partial F^+(\beta)}{\partial \beta}\right|_{\beta=-j\beta_o}} e^{-j\beta_o z}$$

$$- e^{-j\gamma_o z} + \text{Branch cut integral} \qquad (28)$$

The first term in equation (28) represents the TM_0 surface wave mode in the open portion of the structure. The second term is the portion of the scattered field that nullifies the incident field in the region $z > 0$.

Continuous spectrum. - The branch cut integral or continuous portion of the spectrum gives rise to the waves associated with the radiation field. The pattern of the far zone radiation field will be determined by the method of saddle point integration. In the region $r > b$ the scattered field is given by

$$\psi_s(r,z) = \frac{1}{2\pi j} \int_C \varphi(b^+,\beta) \frac{H_1^2\left(\sqrt{k_o^2 + \beta^2}\, r\right)}{H_1^2\left(\sqrt{k_o^2 + \beta^2}\, b\right)} e^{\beta z}\, d\beta$$

where $\varphi(b^+,\beta)$ is given by equation (26). At this point, it is convenient to map the complex β-plane into the complex ν-plane with the mapping function

$$\beta = -jk_o \sin \nu$$

with $\nu = \sigma + j\eta$ and to transform r and z into their spherical coordinate equivalents with $r = \rho \cos \varphi$ and $z = \rho \sin \varphi$ (see fig. 1). The complex ν-plane is shown in figure 4, where the entire β-plane is mapped into a strip of width π in the ν-plane. The quantities Q_1 to Q_4 refer to the images of the quadrants of the β-plane in the ν-plane. With this transformation the expression for the scattered magnetic field becomes

$$\psi_s(\rho,\varphi) = -\frac{1}{2\pi j} \int_C \frac{H_1^2(k_o\rho \cos \varphi \cos \nu) F^-(-j\gamma_o) e^{-jk_o\rho \sin \varphi \sin \nu}}{H_0^2(k_o b \cos \nu) F^+(-jk_o \sin \nu)(\gamma_o - k_o \sin \nu)}\, d\nu \qquad (29)$$

If the observation angle φ is selected such that $\cos \varphi \neq 0$, then for $k_o\rho \gg 1$ the Hankel function $H_1^2(k_o\rho \cos \varphi \cos \nu)$ in equation (29) can be replaced by its asymptotic form

$$H_1^2(k_o\rho \cos \varphi \cos \nu) \simeq \sqrt{\frac{2}{k_o\rho\pi \cos \varphi \cos \nu}}\, e^{-j\left(k_o\rho \cos \varphi \cos \nu - \frac{3\pi}{4}\right)}$$

where terms of the order of $(k_o\rho)^{-3/2}$ and lower have been neglected. The scattered field is then given by

$$\psi_s(\rho,\varphi) = -\frac{1}{2\pi j} \int_C \frac{2^{1/2} F^-(-j\gamma_o) e^{-j\left(k_o\rho \cos(\nu - \varphi) - \frac{3\pi}{4}\right)}}{H_0^2(k_o b \cos \nu) F^+(-jk_o \sin \nu)(\gamma_o - k_o \sin \nu)(k_o\rho\pi \cos \varphi \cos \nu)^{1/2}}\, d\nu \qquad (30)$$

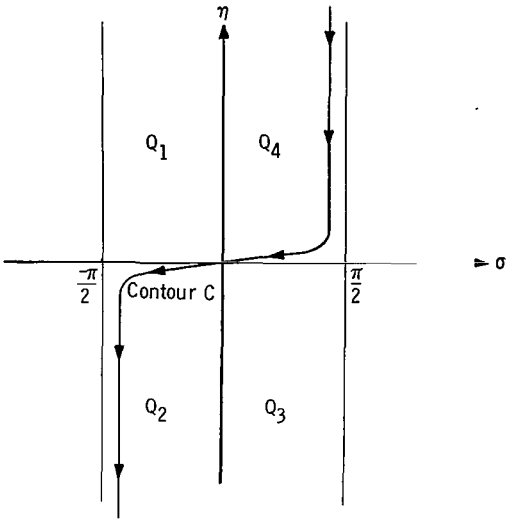

Figure 4. - Inversion contour in complex ν-plane.

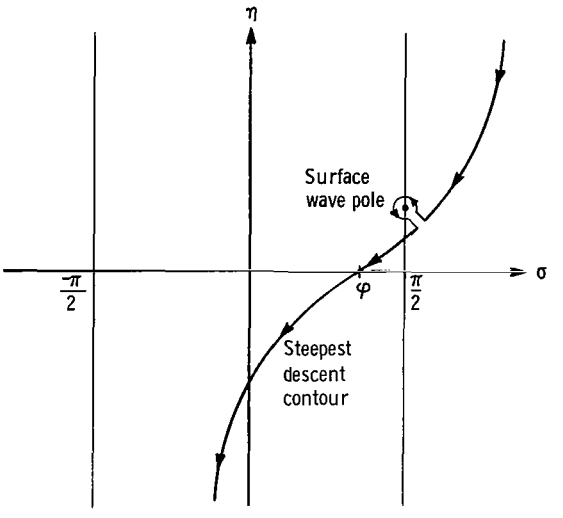

Figure 5. - Steepest descent contour in complex ν-plane.

for $k_o\rho \gg 1$. The integral will be evaluated by deforming the contour C into the contour of steepest descent. The exponential term in equation (30) contains a saddle point where $\sin(\nu - \varphi) = 0$ or where $\nu = \varphi$. In the vicinity of the saddle point, the quantity $\cos(\nu - \varphi)$ can be expanded in a Taylor series to give

$$\cos(\nu - \varphi) = 1 - \frac{\zeta^2}{2} \sin \xi \cos \xi \ . \ . \ .$$

where $\zeta e^{j\xi} = \nu - \varphi$. The imaginary part of $\cos(\nu - \varphi)$ will have its greatest rate of change along the contour that passes through the saddle point $\nu = \varphi$ at an angle of $\pi/4$ with the σ axis and, in general, satisfies the equation $\mathrm{Re}[k_o \cos(\nu - \varphi)] = \mathrm{Re}\ k_o$. This steepest descent contour (SDC) is shown in figure 5. The exponential term in equation (30) has unit modulus at the saddle point $\nu = \varphi$ and falls off as $e^{-(k_o\rho/2)\zeta^2}$ with distance ζ along the steepest descent contour. If $k_o\rho \gg 1$, the dominant portion of the integral for $\psi_s(\rho,\varphi)$ will be the integrand evaluated at $\nu = \varphi$ times the integral of the Gaussian term with respect to ρ. Performing the integration gives

$$\psi_s(\rho,\varphi) = \frac{F^-(-j\gamma_o)e^{-j(k_o\rho+\pi/2)}}{\pi F^+(-jk_o \sin\varphi)H_0^2(k_o b \cos\varphi)(\gamma_o - k_o \sin\varphi)(k_o\rho \cos\varphi)} \qquad (31)$$

If more terms were retained in the asymptotic expansion of the Hankel function and in the expansion of the exponent in equation (28), $\psi_s(\rho,\varphi)$ would contain additional terms of the order of $(k_o\rho)^{-3/2}$ and lower. These additional terms would give a better approximation to the field, especially if $k_o\rho$ is not extremely large, but they would not contribute to any net radiated power.

In deforming the contour C into the steepest descent contour, some of the poles of the integrand may be crossed as shown in figure 5. This usually

happens if the observation angle is near $\pi/2$. It simply indicates that near the reactive surface the total field also consists of the discrete surface wave modes.

This completes the formal solution for the scattered magnetic field. The total field can now be found by adding the scattered field to the incident field as given by equation (7).

ENERGY TRANSPORTED BY FIELD

The energy transported by the field will be computed by using the complex Poynting vector theorem. The only components of the total field that transport energy are the TM_{oo} incident field (eq. (7)), the TM_{oo} reflected field (the first term in eq. (27)), the TM_o surface wave field (the first term in eq. (28)), and the far zone radiation field (eq. (31)).

Since the function $\psi(r,z)$ is the θ component of the total magnetic field, the electromagnetic field $\bar{E},\bar{H}$ is given by

$$\vec{E} = \frac{1}{j\omega\epsilon_o} \nabla x\psi\vec{a}_\theta$$

$$\vec{H} = \psi\vec{a}_\theta$$

Thus, the power P associated with the total field is

$$P = \frac{1}{2} \mathrm{Re} \int_S \vec{E}x\vec{H}^* \cdot d\vec{S} = \frac{1}{2\omega\epsilon_o} \mathrm{Im} \int_S (\nabla x\psi\vec{a}_\theta)x\psi^*\vec{a}_\theta \cdot d\vec{S}$$

where S denotes the surface of suitable cross section of the surface wave structure and ψ^* denotes the complex conjugate of ψ.

For the case of the incident, reflected, and surface wave fields, the only component of the curl of $\psi\vec{a}_\theta$ that is of interest is the radial component given by $-\partial\psi/\partial z$. Since

$$-\frac{\partial\psi_i}{\partial z} = j\gamma_o\psi_i$$

$$-\frac{\partial\psi_{rf}}{\partial z} = -j\gamma_o\psi_{rf}$$

$$-\frac{\partial \psi_{sw}}{\partial z} = j\beta_o \psi_{sw}$$

the respective powers are

$$P_i = \frac{\pi \gamma_o}{\omega \epsilon_o} \int_a^b |\psi_i|^2 \, r \, dr$$

$$P_{rf} = \frac{\pi \gamma_o}{\omega \epsilon_o} \int_a^b |\psi_{rf}|^2 \, r \, dr$$

$$P_{sw} = \frac{\pi \beta_o}{\omega \epsilon_o} \int_a^\infty |\psi_{sw}|^2 \, r \, dr$$

where the subscripts i, rf, and sw refer to the incident, reflected, and surface wave portions of the total field, respectively. For the case of the far zone radiation field, the component of the curl of $\psi \vec{a}_\theta$ that is of interest is the φ component given by $\frac{1}{\rho} \frac{\partial}{\partial \rho} (\rho \psi)$. Actually, only the portion of this component that varies as ρ^{-1} is of interest. Thus,

$$\frac{1}{\rho} \frac{\partial}{\partial \rho} (\rho \psi) \simeq -jk_o \psi$$

for $k_o \rho \gg 1$. The radiated power is, therefore,

$$P_{rad} = \frac{\pi k_o}{\omega \epsilon_o} \int_{-\pi/2}^{\pi/2} |\psi_{rad}|^2 \, \rho^2 \cos \varphi \, d\varphi$$

NUMERICAL RESULTS

The powers associated with the various portions of the field were computed on an IBM 7094. Some typical results are shown in figures 6 to 8 for $b/a = 2.3$ and in figures 9 to 11 for $b/a = 10.0$. The values of 2.3 and 10.0 for b/a correspond to characteristic impedances of 50 and 138 ohms, respectively, for a coaxial line with an air dielectric. The ratios of surface wave power, reflected power, and radiated power to incident power are shown as functions of $k_o d$ where $d = b - a$. The range of $k_o d$ is restricted so that only the TM_{oo}

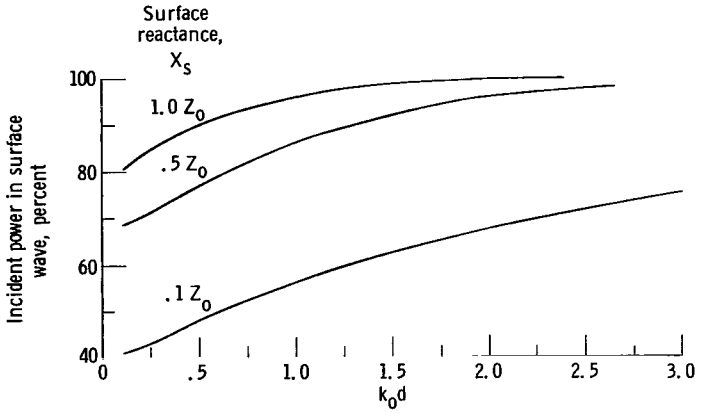

Figure 6. - Percent of incident power in surface wave against k_0d for constant values of surface reactance. Radius ratio, b/a = 2.3.

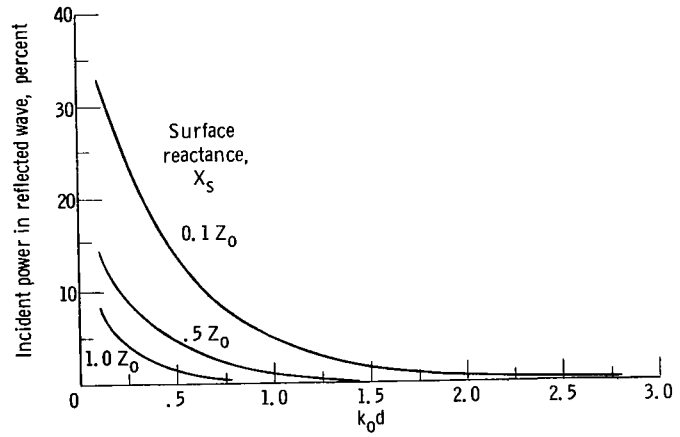

Figure 7. - Percent of incident power in reflected wave against k_0d for constant values of surface reactance. Radius ratio, b/a = 2.3.

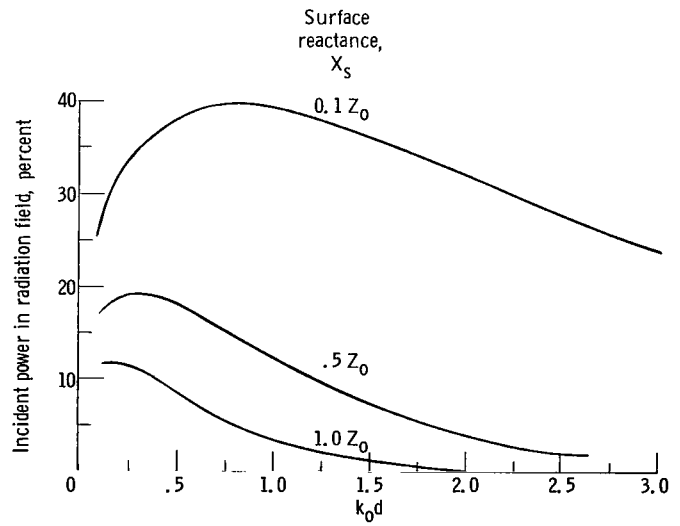

Figure 8. - Percent of incident power in radiated wave against k_0d for constant values of surface reactance. Radius ratio, b/a = 2.3.

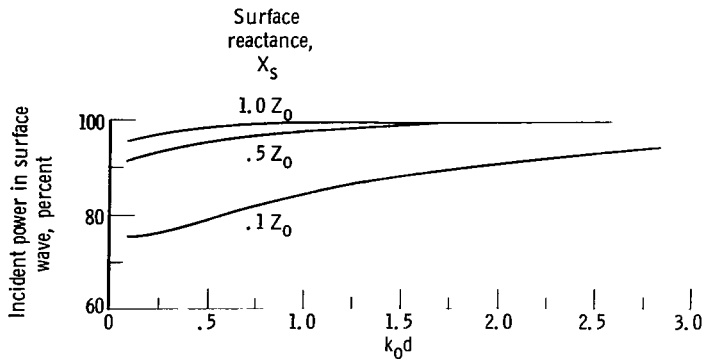

Figure 9. - Percent of incident power in surface wave against k_0d for constant values of surface reactance. Radius ratio, b/a = 10.0.

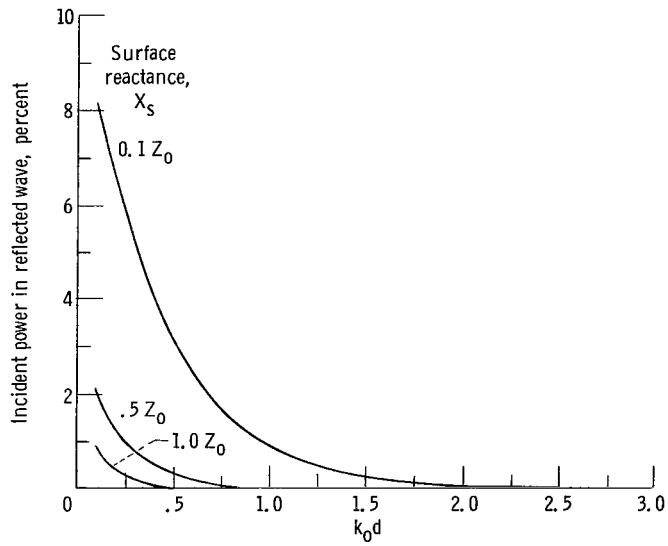

Figure 10. - Percent of incident power in reflected wave against k_0d for constant values of surface reactance. Radius ratio, b/a = 10.0.

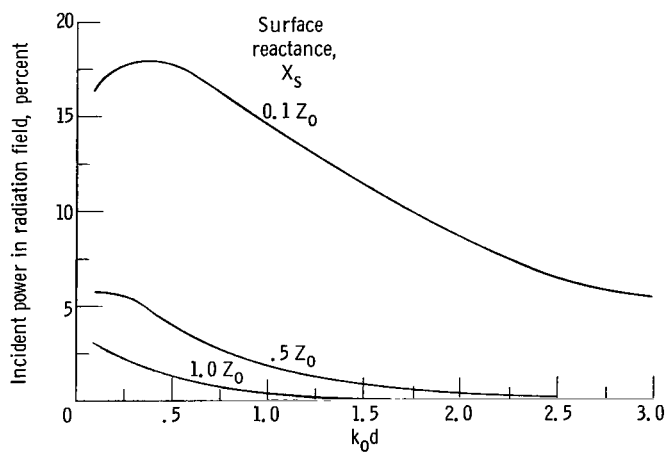

Figure 11. - Percentage of incident power in radiated wave against k_0d for constant values of surface reactance. Radius ratio, b/a = 10.0.

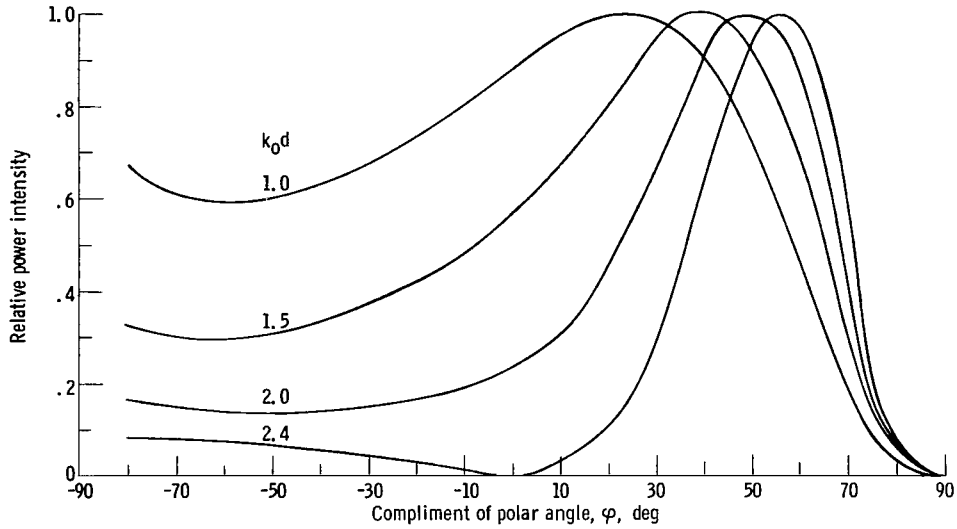

Figure 12. - Radiation pattern. Surface reactance, $X_s = 1.0\ Z_0$; radius ratio, b/a = 2.3.

mode will propagate in the coaxial portion of the structure. The results show that this structure is very efficient in launching surface waves, even when the surface reactance is quite low, if k_0d is not too small. A comparison of figures 6 and 9 shows that the larger value of b/a yields a higher launching efficiency for a given value of k_0d.

The launcher is also very broad banded as evidenced by the small reflected power over a large range of k_0d. It should be noted that the curves shown in figures 6 to 11 are for constant values of surface reactance. In practice, the surface reactance will be a function of frequency so that the actual bandwidth of the launcher will not be known until the surface wave structure is specified.

The radiation pattern of the far zone field is shown in figure 12 for the case where $b/a = 2.3$ and $X_s = Z_0$. The curves have been normalized by setting the maximum value of the power density in the forward direction equal to 1. The radiation patterns for other values of surface reactance are quite similar to those shown in figure 12. When surface reactance was increased, the beam width was found to become slightly smaller for a fixed value of k_0d.

Since the energy transported by the total field is conserved, the power associated with the incident wave must always equal the sum of the powers associated with the reflected wave, the surface wave, and the radiation field. This fact was used to check the numerical results.

LAUNCHING EFFICIENCY-APPROXIMATION TECHNIQUES

A common method for determining the quality of a surface wave launcher is to compute its launching efficiency as a function of frequency. The launching efficiency is defined as the ratio of the surface wave power to the total power radiated from the aperture of the launcher. Before presenting numerical values for the launching efficiency by using the results from the exact analysis, it is

instructive to consider two approximation techniques. This problem provides an excellent opportunity to check the validity of these techniques since an exact result has already been obtained.

The first technique that will be considered is to approximate the aperture distribution of the launcher with a chopped surface wave distribution. In the plane $z = 0$ the total field $\psi(r,o)$ is assumed to be given by

$$\psi(r,o) = H_1^2(-jh_o r) \qquad \text{for} \quad a < r < b$$

$$\psi(r,o) = 0 \qquad \text{for} \quad r > b$$

The total power radiated from the aperture is, therefore,

$$P_{total} = \frac{\pi\beta_o}{\omega\epsilon_o} \int_a^b |H_1^2(-jh_o r)|^2 r \, dr$$

The surface wave field that is excited by this aperture distribution is of the form

$$B_o H_1^2(-jh_o r) e^{-j\beta_o z}$$

The amplitude of the surface wave B_o can be computed by using the orthogonal properties of the surface wave modes (ref. 4).

$$B_o = \frac{\int_a^b |H_1^2(-jh_o r)|^2 r \, dr}{\int_a^\infty |H_1^2(-jh_o r)|^2 r \, dr}$$

The definition of launching efficiency shows that the efficiency of this aperture distribution is equal to B_o. Since the launching efficiency is equal to the ratio of two integrals with each integral having the same integrand and same lower limit, the launching efficiency can be made arbitrarily close to 100 percent by increasing the upper limit b of the integral in the numerator. This illustrates the requirement of an infinitely large aperture before 100 percent efficiency can be obtained.

A second approximation technique that will be considered is Kirchhoff's approximation. For this method, the aperture distribution is approximated by the unperturbed incident field; that is, the total field $\psi(r,z)$ evaluated at the aperture plane $z = 0$ is approximated by

$$\psi(r,o) = \psi_i(r,o) \qquad \text{for} \quad a < r < b$$

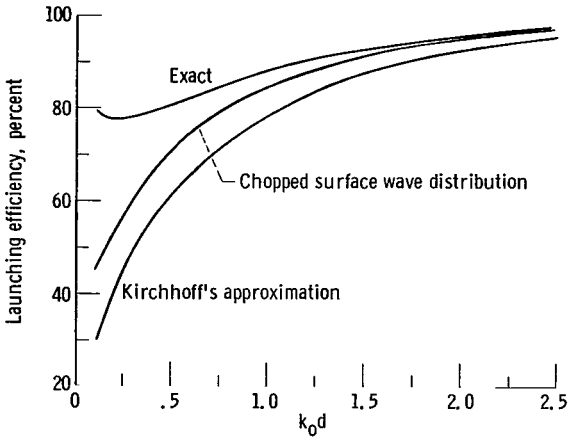

Figure 13. - Launching efficiency against k_0d. Surface reactance, $X_s = 0.5$; radius ratio, $b/a = 2.3$.

$$\psi(r,o) = 0 \qquad \text{for} \quad r > b$$

where $\psi_i(r,z)$ is given by equation (7).

For this distribution, the total power radiated from the aperture is

$$P_{total} = \frac{\pi\gamma_o}{\omega\epsilon_o} \int_a^b |\psi_i(r,o)|^2 r \, dr$$

The surface wave excited by this distribution is of the form

$$B_o H_1^2(-jh_o r) e^{-j\beta_o z}$$

where the amplitude B_o is given by

$$B_o = \frac{\displaystyle\int_a^b |\psi_i(r,o) H_1^2(-jh_o r)| r \, dr}{\displaystyle\int_a^\infty |H_1^2(-jh_o r)|^2 r \, dr}$$

The launching efficiency is therefore

$$\frac{\beta_o \left| \displaystyle\int_a^b \psi_i(r,o) H_1^2(-jh_o r) r \, dr \right|^2}{\gamma_o \displaystyle\int_a^\infty |H_1^2(-jh_o r)|^2 r \, dr \int_a^b |\psi_i(r,o)|^2 r \, dr}$$

Schwarz's inequality requires the ratios of the integrals to be less than unity. Thus, the launching efficiency is bounded from above by β_o/γ_o.

Numerical values for the launching efficiency, showing both the exact and approximate, are presented in figure 13. The results show that the launcher is very efficient over a large range of frequencies even if the surface reactance is quite low. The exact results always give a higher launching efficiency than that predicted by any of the approximate techniques; however, the approximation techniques give quite accurate results for $k_0d > 1$. The values of k_0d when the approximations fail also give a large reflected power as shown in figure 7. The launcher would not be useful in this range unless some impedance matching

techniques were employed. For all cases, the chopped surface wave approximation proved to be more accurate than Kirchhoff's method in giving an estimate of of the exact launching efficiency.

CONCLUSIONS

Numerical results were obtained for the energy transported by the reflected, the surface wave, and the radiation fields by using an exact analysis. The results show that the coaxial launcher is very efficient in exciting surface waves even when the surface reactance is quite low. Both approximation techniques gave quite accurate results as long as the frequency was sufficiently high. Large discrepancies between the exact and approximate results occurred only when the launching efficiency was low.

Lewis Research Center,
National Aeronautics and Space Administration,
Cleveland, Ohio, October 25, 1965.

APPENDIX - WIENER-HOPF FACTORIZATION

The Wiener-Hopf factorization of the function $F(\beta)$ consists of finding two functions $F^+(\beta)$ and $F^-(\beta)$ such that $F(\beta) = F^+(\beta)/F^-(\beta)$, where $F^+(\beta)$ is analytic and nonzero in the region $\text{Re}\ \beta > -\gamma_o''$ and $F^-(\beta)$ is analytic and nonzero in the region $\text{Re}\ \beta < \gamma_o''$. The formal procedure for performing this factorization is based on the Cauchy integral formula (ref. 5, pp. 987-989).

Consider Cauchy's integral formula

$$f(\beta) = \frac{1}{2\pi j}\int_C \frac{f(s)}{s - \beta}\, ds$$

where β is a point interior to C and $f(s)$ is single-valued and analytic within and on C. Let the contour C be of the form shown in figure 14. The contributions to the integral along C_2 and C_4 cancel. Thus,

$$f(\beta) = \frac{1}{2\pi j}\int_{C_1} \frac{f(s)}{s - \beta}\, ds + \frac{1}{2\pi j}\int_{C_3} \frac{f(s)}{s - \beta}\, ds$$

The integration over C_1 produces a function that is analytic everywhere interior to C_1, whereas the integration over C_3 produces a function that is analytic everywhere exterior to C_3. This procedure allows an arbitrary function to be decomposed into the sum of two functions with each function being analytic in different but overlapping portions of the complex plane.

The same idea can be extended to the case where $f(\beta)$ is analytic in an infinitely long strip. If $f(\beta)/\beta$ vanishes as $|\beta| \to \infty$, $f(\beta)$ can be decomposed into the sum of two functions $f^+(\beta)$ and $f^-(\beta)$ by performing the indicated integrations over C_1 and C_3 in figure 15.

$$f(\beta) = f^+(\beta) + f^-(\beta)$$

$$f^-(\beta) = \frac{1}{2\pi j}\int_{C_1} \frac{f(s)}{s - \beta}\, ds$$

$$f^+(\beta) = \frac{1}{2\pi j}\int_{C_3} \frac{f(s)}{s - \beta}\, ds$$

The function $f^-(\beta)$ is analytic for $\text{Re}\ \beta < s_1$, and $f^+(\beta)$ is analytic for $\text{Re}\ \beta > s_2$. If $f(\beta)$ is an even function of β, the functions $f^+(\beta)$ and $f^-(\beta)$ are related by $f^+(-\beta) = f^-(\beta)$ and $f^+(\beta) = f^-(-\beta)$. This relation provides a

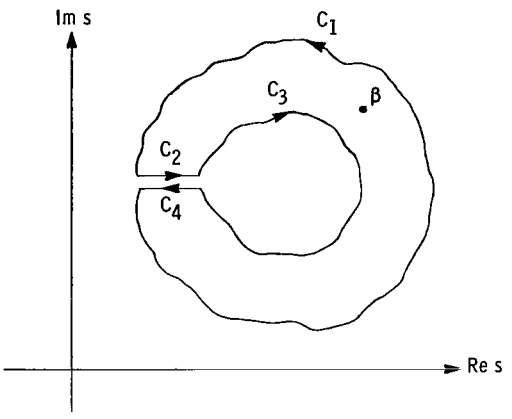

Figure 14. - Contour C in complex s-plane.

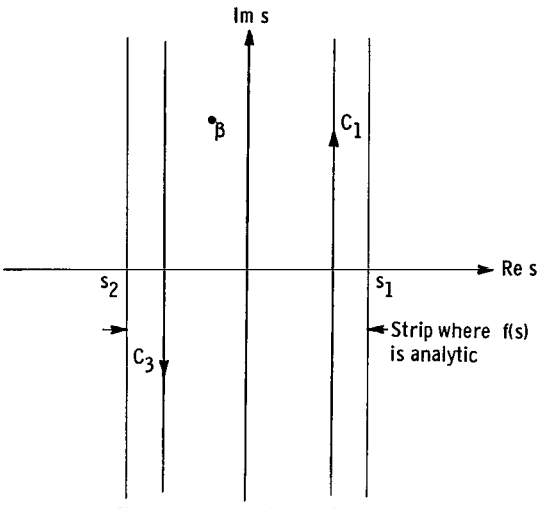

Figure 15. - Complex s-plane.

very simple method for computing $f^+(\beta)$, for example, if $f^-(\beta)$ is known.

In the problem under consideration, it is necessary to decompose the function $F(\beta)$ into the ratio of two functions $F^+(\beta)$ and $F^-(\beta)$ rather than into the sum of two functions, as discussed in the preceding paragraphs. The desired decomposition is easily carried out if the function $\ln F(\beta)$ is identified with $f(\beta)$. Since

$$\ln F(\beta) = \ln F^+(\beta) - \ln F^-(\beta)$$

and

$$f(\beta) = f^+(\beta) + f^-(\beta)$$

it follows that

$$F^+(\beta) = e^{f^+(\beta)}$$

$$F^-(\beta) = e^{-f^-(\beta)}$$

where $f^+(\beta)$ and $f^-(\beta)$ are computed with $f(\beta) = \ln F(\beta)$ by using the previously developed formulas. Since $F(\beta)$ is an even function of β, $F^+(\beta)$ and $F^-(\beta)$ are related by $F^+(\beta)F^-(-\beta) = 1$ and $F^+(-\beta)F^-(\beta) = 1$.

Because of the complexity of the function $F(\beta)$ in the problem under consideration, it is convenient to consider the various portions of the function separately. The function $F(\beta)$ will be expressed, for convenience, as the product of the functions $K(\beta)$, $L(\beta)$, $M(\beta)$, $N(\beta)$, and $(\beta^2 + \gamma_o^2)^{-1}$ (see eq. (21)), where

$$K(\beta) = \frac{2j}{\pi b \lambda}$$

$$L(\beta) = \frac{H_0^2(\lambda a)}{H_0^2(\lambda b)}$$

$$M(\beta) = \lambda + \alpha \frac{H_1^2(\lambda a)}{H_0^2(\lambda a)}$$

$$N(\beta) = \frac{\beta^2 + \gamma_o^2}{\lambda^2\left[H_0^2(\lambda a)J_0(\lambda b) - H_0^2(\lambda b)J_0(\lambda a)\right] + \lambda\alpha\left[H_1^2(\lambda a)J_0(\lambda b) - H_0^2(\lambda b)J_1(\lambda a)\right]}$$

and

$$\lambda = (k_o^2 + \beta^2)^{1/2}$$

First, consider the function $L(\beta) = L^+(\beta)/L^-(\beta)$. The factor $L^-(\beta)$ is given by

$$L^-(\beta) = e^{-\lambda^2 l^-(\beta)}$$

where

$$l^-(\beta) = \frac{1}{2\pi j} \int_{C_1} \frac{\ln\left[\frac{H_0^2(\Omega a)}{H_0^2(\Omega b)}\right]}{\Omega^2(s - \beta)}\, ds$$

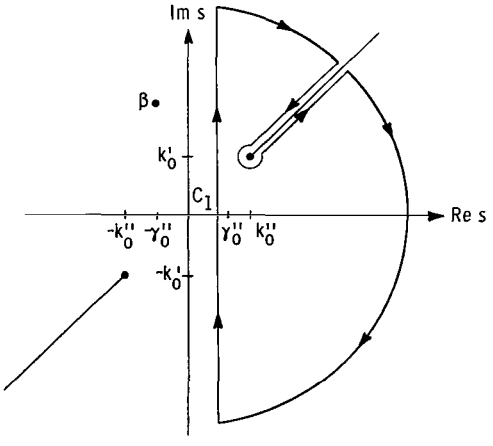

Figure 16. - Contour C_1 in complex s-plane.

and

$$\Omega = (k_o^2 + s^2)^{1/2}$$

It is necessary to include a convergence factor Ω^{-2} in the expression for $l^-(\beta)$ since the function $L(\beta)$ does not have the proper behavior at infinity. The contour C_1 must be located in the strip $-\gamma_o'' < \text{Re } s < \gamma_o''$ as shown in figure 16 with the point $s = \beta$ located to the left of C_1.

The integral over C_1 can be evaluated by using Cauchy's residue theorem. The contour can be closed in the right half s plane with a semicircle of infinite radius that is deformed around the branch cut. It can be

shown, after a considerable amount of work, that the integral over the semicircle of infinite radius and over the circle of infinitesimal radius that encloses the branch point $s = jk_o$ is zero. Since the integrand has no poles in the right half β plane (ref. 8), the integral over C_1 is equal to the branch cut integral. The branch cut integral can be simplified by introducing a new real variable of integration x such that $s = jk_o x$. The branch cut corresponds to the range in x of $1 \leq x < \infty$. After some manipulations, the expression for $L^-(\beta)$ becomes

$$L^-(\beta) = \exp\left\{ \frac{(\beta^2 + k_o^2)}{2\pi k_o} \text{ P.V.} \int_1^\infty \frac{\ln\left[\frac{H_0^2\left(-jk_o a \sqrt{x^2 - 1}\right) H_0^2\left(jk_o b \sqrt{x^2 - 1}\right)}{H_0^2\left(jk_o a \sqrt{x^2 - 1}\right) H_0^2\left(-jk_o b \sqrt{x^2 - 1}\right)} \right]}{(x^2 - 1)(jk_o x - \beta)} dx \right\}$$

where P.V. denotes the principal value of the integral. The factor $L^+(\beta)$ is given by $L^+(\beta) = 1/L^-(-\beta)$ since $L(\beta)$ is an even function of β.

Next, consider the function $M(\beta) = M^+(\beta)/M^-(\beta)$. The factorization can be performed on this function by taking the logarithmic derivative of $M(\beta)$:

$$\ln M^+(\beta) - \ln M^-(\beta) = \ln M(\beta)$$

$$\frac{1}{M^+(\beta)} \frac{d}{d\beta} M^+(\beta) - \frac{1}{M^+(\beta)} \frac{d}{d\beta} M^-(\beta) = \frac{1}{M(\beta)} \frac{d}{d\beta} M(\beta)$$

Thus

$$M^-(\beta) = M^-(0) \exp \int_0^\beta \left[-\frac{1}{2\pi j} \int_{C_1} \frac{m(s)}{s - \beta} ds \right] d\beta$$

where

$$m(\beta) = \frac{1}{M(\beta)} \frac{d}{d\beta} M(\beta)$$

The integral over C_1 can be evaluated by closing the contour in the right half β plane with a semicircle of infinite radius that is deformed around the branch cut as shown in figure 16. It can be shown that the integral over this semicircle vanishes. Thus, the integral over the contour C_1 is equal to $2\pi j$ times the sum of the residues of the enclosed poles of $m(s)$ plus the branch cut integral. The integrand $m(s)$ has a pole at $s = j\beta_o$ and

a second pole at the branch point $s = jk_o$. After some manipulation it can be shown that

$$M^-(\beta) = M^-(0)\exp\left\{\int_0^\beta \left[\frac{1}{2(\beta - jk_o)} - \frac{1}{\beta - j\beta_o}\right]d\beta + \int_0^\beta \text{Branch cut integral } d\beta\right\}$$

The branch cut integral can be simplified by defining a new real variable of integration x such that $s = jk_o x$ as was done for the case of $L^-(\beta)$. The expression for $M^-(\beta)$ then becomes

$$M^-(\beta) = M^-(0)\exp\left\{\int_0^\beta \left[\frac{1}{2(\beta - jk_o)} - \frac{1}{\beta - j\beta_o}\right]d\beta - \frac{k_o}{2\pi}\,\text{P.V.}\int_0^\beta\left[\int_1^\infty \frac{(m^+(x) - m^-(x))dx}{jk_o x - \beta}\right]d\beta\right\}$$

where

$$m^\pm(x) = \left(\frac{jk_o x a^2}{\mp\xi}\right)\left[\mp\xi - \alpha a\,\frac{H_1^2(\mp\xi)}{H_0^2(\mp\xi)}\right]^{-1}\left\{1 + \alpha a \pm \frac{\alpha a}{\xi}\,\frac{H_1^2(\mp\xi)}{H_0^2(\mp\xi)} + \alpha a\left[\frac{H_1^2(\mp\xi)}{H_0^2(\mp\xi)}\right]^2\right\}$$

and

$$\xi = jk_o a\sqrt{x^2 - 1}$$

The factor $M^+(\beta)$ can be easily obtained from $M^-(\beta)$ by using the relation $M^+(\beta) = 1/M^-(-\beta)$ since $M(\beta)$ is an even function of β.

The function $K(\beta) = K^+(\beta)/K^-(\beta)$ can be factored by inspection.

$$K^-(\beta) = \left(\frac{\pi b}{2j}\right)^{1/2}(\beta - jk_o)^{1/2}$$

Again, $K^+(\beta)$ is given by $K^+(\beta) = 1/K^-(-\beta)$ since $K(\beta)$ is an even function of of β.

The function $N(\beta) = N^+(\beta)/N^-(\beta)$ can be factored by expressing it in the form of an infinite product. This is possible since $N(\beta)$ is an even function of $(k_o^2 + \beta^2)^{1/2}$ and has singularities in the form of simple poles (ref. 5,

pp. 382 to 385). From the infinite product expression for $N(\beta)$, the function $N^-(\beta)$ can be easily identified as

$$N^-(\beta) = \sqrt{\frac{2j\alpha}{p_o^2 \pi a}} \prod_{n=1}^{\infty} \left(\frac{\gamma_n - \beta}{p_n} \right) e^{\beta d/n\pi}$$

The function $N^+(\beta)$ is equal to $1/N^-(-\beta)$ since $N(\beta)$ is an even function of β.

The remaining term $(\beta^2 + \gamma_o^2)^{-1}$ in the expression for $F(\beta)$ can easily be factored by inspection. Thus, the factor $F^-(\beta)$ is simply the product of the expressions found for $K^-(\beta)$, $L^-(\beta)$, etc., and the factor $F^+(\beta)$ is the product of the expressions for $K^+(\beta)$, $L^+(\beta)$, etc. The function $F^+(\beta)$ has a single zero at $\beta = -j\beta_o$, because of the zero of $M^+(\beta)$, plus a branch point at $\beta = -jk_o$, because of the branch points of $K^+(\beta)$, $L^+(\beta)$, and $M^+(\beta)$. The function $F^-(\beta)$ has an infinite number of zeros in the β-plane located at $\beta = j\gamma_o$ and $\beta = \gamma_n (n > 0)$, because of the zeros of $N^-(\beta)$, and a branch point at $\beta = jk_o$, because of the branch points of $K^-(\beta)$, $L^-(\beta)$, and $M^-(\beta)$.

Thus far, the function $F(\beta)$ has been decomposed into the ratio of the two functions $F^+(\beta)$ and $F^-(\beta)$ such that $F^+(\beta)$ is analytic for $\text{Re}\ \beta > -\gamma_o''$ and $F^-(\beta)$ is analytic for $\text{Re}\ \beta < \gamma_o''$. The functions $F^+(\beta)$ and $F^-(\beta)$ are not unique. Both $F^+(\beta)$ and $F^-(\beta)$ can be multiplied by any function $p(\beta)$ that is analytic everywhere in the finite complex β-plane to generate a new set of functions $F^+(\beta)$ and $F^-(\beta)$. The proper function $p(\beta)$ to select is that function that gives the functions $F^+(\beta)$ and $F^-(\beta)$ algebraic behavior at infinity rather than exponential behavior. This selection is necessary to ensure that the field satisfies the proper edge conditions.

A very lengthy and tedious study of the asymptotic forms of $F^+(\beta)$ and $F^-(\beta)$ reveals that the proper function $p(\beta)$ is given by

$$p(\beta) = \exp - \left[\frac{\beta P}{2\pi k_o} + \frac{j\beta d}{2} + \frac{\beta d}{\pi} \ln\left(\frac{k_o d}{2\pi} \right) - \frac{\beta d}{\pi} + \frac{\gamma \beta d}{\pi} \right]$$

where γ is Euler's constant and

$$P = \text{P.V.} \int_1^{\infty} \frac{\ln \left[\dfrac{H_0^2\left(-jk_o a \sqrt{x^2 - 1}\right) H_0^2\left(jk_o b \sqrt{x^2 - 1}\right)}{H_0^2\left(jk_o a \sqrt{x^2 - 1}\right) H_0^2\left(-jk_o b \sqrt{x^2 - 1}\right)} \right] - 2k_o d \sqrt{x^2 - 1}}{x^2 - 1} \, dx$$

REFERENCES

1. Zucker, F. J.: Surface and Leaky-Wave Antennas. Antenna Engineering Handbook, Henry Jasek, ed., McGraw-Hill Book Co., Inc., 1961, Ch. 16.

2. Barlow, H. M.; and Brown, J.: Radio Surface Waves. Clarendon Press (Oxford), 1962.

3. Brown, J.: Some Theoretical Results for Surface Wave Launches. IRE Trans. on Antennas and Propagation, vol. AP-7, Dec. 1959, pp. S169-S174.

4. Collin, Robert E.: Field Theory of Guided Waves. McGraw-Hill Book Co., Inc., 1960, pp. 483-485.

5. Morse, Philip M.: and Feshbach, Herman: Methods of Theoretical Physics. Vol. 1. McGraw-Hill Book Co., Inc., 1953.

6. Wiener, N.; and Hopf, E.: Über eine Klasse Singulärer Integralgleichungen. S. B. Preuss. Akad. Wiss., 1931, pp. 696-706.

7. Noble, Benjamin: Methods Based on the Wiener-Hopf Technique for the Solution of Partial Differential Equations. Pergamon Press, Inc., 1958.

8. Watson, G. N.: A Treatise on the Theory of Bessel Functions. Cambridge Univ. Press (London), 1962, pp. 511-513.

3/22/85

"The aeronautical and space activities of the United States shall be conducted so as to contribute . . . to the expansion of human knowledge of phenomena in the atmosphere and space. The Administration shall provide for the widest practicable and appropriate dissemination of information concerning its activities and the results thereof."

—NATIONAL AERONAUTICS AND SPACE ACT OF 1958

NASA SCIENTIFIC AND TECHNICAL PUBLICATIONS

TECHNICAL REPORTS: Scientific and technical information considered important, complete, and a lasting contribution to existing knowledge.

TECHNICAL NOTES: Information less broad in scope but nevertheless of importance as a contribution to existing knowledge.

TECHNICAL MEMORANDUMS: Information receiving limited distribution because of preliminary data, security classification, or other reasons.

CONTRACTOR REPORTS: Technical information generated in connection with a NASA contract or grant and released under NASA auspices.

TECHNICAL TRANSLATIONS: Information published in a foreign language considered to merit NASA distribution in English.

TECHNICAL REPRINTS: Information derived from NASA activities and initially published in the form of journal articles.

SPECIAL PUBLICATIONS: Information derived from or of value to NASA activities but not necessarily reporting the results of individual NASA-programmed scientific efforts. Publications include conference proceedings, monographs, data compilations, handbooks, sourcebooks, and special bibliographies.

Details on the availability of these publications may be obtained from:

SCIENTIFIC AND TECHNICAL INFORMATION DIVISION

NATIONAL AERONAUTICS AND SPACE ADMINISTRATION

Washington, D.C. 20546